

Dynamics of Water Confined on a TiO₂ (Anatase) Surface[†]

Andrey A. Levchenko,[‡] Alexander I. Kolesnikov,[§] Nancy L. Ross,^{||} Juliana Boerio-Goates,[⊥] Brian F. Woodfield,[⊥] Guangshe Li,^{⊥, #} and Alexandra Navrotsky^{*, ‡}

Peter A. Rock Thermochemistry Laboratory and NEAT ORU, University of California at Davis, Davis, California 95616, Intense Pulsed Neutron Source Division, Argonne National Laboratory, Argonne, Illinois 60439, Department of Geological Sciences, Virginia Polytechnic Institute and State University, Blacksburg, Virginia 24061, and Department of Chemistry and Biochemistry, Brigham Young University, Provo, Utah 84602

Received: July 30, 2007; In Final Form: September 18, 2007

Inelastic neutron scattering has been employed to probe the vibrational density of states of water confined by an oxide surface, namely, nanoparticles of the anatase polymorph of TiO₂. The heat capacity of confined water has been measured by adiabatic calorimetry and compared with values derived from the vibrational density of states. Both inelastic neutron scattering and calorimetry demonstrate restricted mobility and lower heat capacity and entropy of confined water as compared to the bulk.

Introduction

The confinement effects of porous media, nanotubes, and solid surfaces on the dynamics and properties of liquids have attracted much attention due to the large range of new phenomena observed in confined geometry. Examples include polymorphic transformations, slowing down or speeding up of dynamics,^{1–3} and shifts in glass transition and crystallization temperature⁴ induced by confinement. Studies of water confinement are important to fundamental and applied science because of the widespread occurrence and variety of confinement phenomena in nature, such as water mobility in cells and membranes, water and oil transport in rocks, and applications such as controlled drug release.

Water can be present in molecular and/or dissociated forms on oxide surfaces, including those of nanoparticles, and therefore may have a significant effect on the stability and growth of nanoparticles. We have recently confirmed that water, confined by a TiO₂ surface, cannot be removed completely from nanoparticles without grain growth, implying, perhaps, that it plays a major role in stabilizing the nanoparticles.^{5–7} In this study, we examine how surface confinement influences water vibrations and heat capacity, as measured by inelastic neutron scattering (INS) and adiabatic calorimetry.

On the basis of rather scattered studies of metals,^{8–15} alloys,^{16,17} and a few binary oxides,^{18,19} it was concluded that the heat capacity of nanoparticles is higher than that of the bulk. This supports intuition that atoms near the surface are bound less tightly. We have measured the specific heats of TiO₂ anatase and rutile nanoparticles.⁷ By successively reducing the water content without changing the particle size, and measuring the water content and heat capacity, we could separate effects of

water from those of particle size. In contrast to the prevailing belief that nanoparticles have higher heat capacities, we observed that heat capacities of anatase and rutile nanoparticles in the low temperature range of 15–350 K are not significantly different from those of the bulk, when proper corrections for water are made.⁷ In view of this detailed study of heat capacity, water confined by the TiO₂ surface is an excellent system to study dynamics and energetics by other complementary methods.

Our recent study⁶ has shown that, reflecting a strong interaction of water with the TiO₂ surface, its heat capacity and entropy appear to be somewhat smaller than that of bulk ice as evidenced by water adsorption measurements. This might be surprising if one expects higher heat capacities and entropies of water due to disordering and/or mobility at the interface.

Because of the large incoherent neutron scattering cross-section of hydrogen as compared to other elements, the INS techniques can give substantial insight into the structure, vibrational density of states (VDOS), and overall dynamics of water on the surface. Using appropriate models, the heat capacity of confined water can be calculated from the VDOS. There are a few neutron scattering studies of water in confined geometry in nanotubes,³ porous media,^{20–24} and oxides.^{1,2,21,25,26} To the best of our knowledge, there are only two papers^{25,27} that identified the VDOS of water adsorbed on oxide nanoparticles, namely, rare-earth modified zirconium oxide. These studies showed that the VDOS is sensitive to hydrogen bonding and motion of water molecules.

For this study, we have chosen anatase nanoparticles as a model system for several reasons. The TiO₂ nanoparticles (7 nm in size), recently synthesized and characterized by us,^{5,6} have a spherical shape and crystallize in the anatase phase. It has been shown experimentally that anatase is the stable polymorph of TiO₂ at the nanoscale level.^{5,6} Thus, these particles are well-characterized and unlikely to decompose or degrade during further experimentation at and below room temperature.

The goal of this study is three-fold. First, we measured the heat capacities of confined and bulk water on the nanoparticle surfaces utilizing low temperature adiabatic calorimetry. Second,

[†] Part of the "Giacinto Scoles Festschrift".

* Corresponding author. E-mail: anavrotsky@ucdavis.edu.

[‡] University of California at Davis.

[§] Argonne National Laboratory.

^{||} Virginia Polytechnic Institute and State University.

[⊥] Brigham Young University.

[#] Present address: State Key Structural Chemistry Laboratory, Fujian Institute of Research on the Structure of Matter, Graduate School of Chinese Academy of Sciences, Fuzhou 350002, People's Republic of China.

we calculated the VDOS based on INS data and computed the heat capacity for water confined on the surface of TiO₂ (anatase) nanoparticles. Third, we compared the calculated heat capacities of confined and bulk hexagonal ice (ice Ih) with the measured specific heats obtained by low temperature adiabatic calorimetry. The heat capacities of TiO₂ nanoparticles have been reported by us before.⁷ This is the first report of INS measurements and comparison and interpretation of both data sets to gain insight into the dynamics of water confinement on the anatase surface.

Experimental Procedures

Sample Preparation and Characterization. A sol-gel method as reported previously⁵ was used to obtain high quality spherical anatase nanoparticles. Briefly, TiCl₄ was added slowly to ice cooled ethanol with stirring. The sol thus formed was allowed to remain in air for several hours and then was heated at 358 K until it became white powder. Powder with extremely low impurities was achieved by a large number of washings of the reaction product in a centrifuge at room temperature. The resulting white powder was dried in an oven at 353 K in air and used for further analysis. The only impurities found were carbon and chlorine, but both were only at the part per million level.

The specific surface area of the material was measured to be 198 m²/g according to the Brunauer-Emmett-Teller (BET) equation^{28,29} from N₂ adsorption at 77 K in a relative pressure range $p/p^\circ = 0.05-0.3$ ($p^\circ =$ saturation pressure) using a Micromeritics ASAP 2020 surface area and porosity analyzer. Before the BET measurement, the sample was degassed at 373 K for at least 10 h after a stable static vacuum of 3×10^{-3} Torr was reached.

The water content of sample was determined by thermogravimetric analyses (TGA) on a 30 mg pellet using a Netzsch STA 449 system and checked by weighing the pellet before and after heating at 1273 K for 2 h. The phase purity and particle size of anatase nanoparticles were checked by X-ray diffraction (XRD) and transmission electron microscopy (TEM) as reported elsewhere.⁵ The particle sizes determined by XRD and TEM agree with the BET results within 1 nm.

Neutron Scattering Experiments. INS experiments were conducted on a 6.3 g sample of 7 nm anatase nanoparticles using the high resolution medium energy chopper spectrometer (HRMECS) at IPNS. HRMECS is a direct geometry time-of-flight machine. The incoming neutrons have a fixed energy E_i , selected by a rotating chopper, and the energies of scattered neutrons are derived from time-of-flight for neutrons arriving at the detector. Under optimum conditions (large E_i and small scattering angles), the neutron momentum transfers at high energy transfers are relatively small, which makes it possible to measure good quality INS spectra up to the highest excitation energy of interest. The incident energies, 50, 150, and 600 meV, were used to measure vibrational spectra at 4 K over the 0–550 meV range with a resolution between 2 and 3% of the incident neutron beam energy. The momentum transfer range covered in these measurements was 0.75–8.4 Å⁻¹ depending on the incident energy, energy transfer, and scattering angle.

To calculate the VDOS for water, INS spectra $g(E)$ were corrected for multiphonon and sample holder scattering. The overall effect of multiphonon scattering, calculated in this study in a harmonic isotropic approximation using an iterative technique,³⁰ is small because HRMECS provides relatively low momentum transfer Q . Indeed, two-phonon neutron scattering is proportional to Q^4 , so the multiphonon contribution in our case is an order of magnitude smaller than that in bulk ice

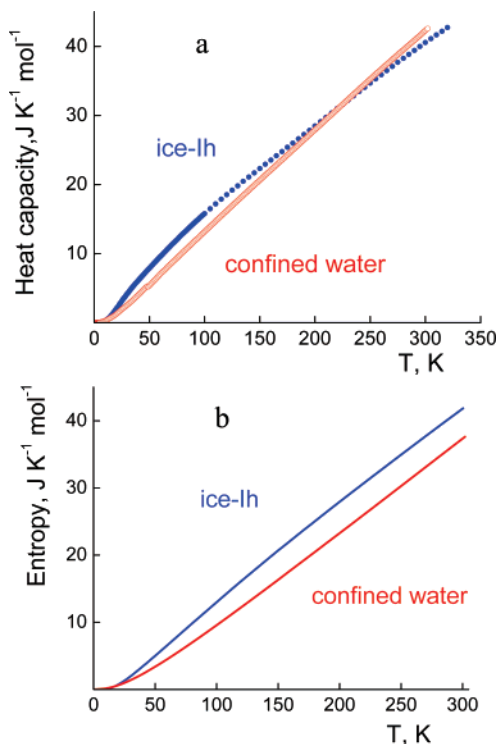


Figure 1. Heat capacity C_p for bulk ice-Ih and water confined on 7 nm anatase obtained by low temperature adiabatic calorimetry.

experiments of Klug et al.,³¹ in which the multiphonon correction is a central issue. Neutron absorption and self-shielding effects are negligible. We believe that, for water confined on the anatase surface, the main contribution to uncertainties in $g(E)$ comes from overlapping translational and librational bands in the confined water spectrum as discussed next.

Heat Capacity Measurements. The heat capacity measurements from 15 to 350 K with an absolute accuracy of better than $\pm 0.2\%$ from 30 to 350 K and better than $\pm 1\%$ below 30 K were performed using a custom-built adiabatic calorimeter described in detail previously.³² To obtain water heat capacities, the specific heat of a dry anatase sample with relatively large crystal grains (bulk sample) was also measured and subtracted from the data for anatase nanoparticles containing known amounts of water. The sample used for heat capacity measurements had a coverage of 1.7×10^{-5} mol of H₂O/m², similar to the amount of water on the sample surface in the INS experiments (1.5×10^{-5} mol of H₂O/m²).

Results

Heat Capacity. As nanoparticles become smaller, their specific heat (per gram of sample) increases. Boerio-Goates et al.⁷ examined a correlation between the apparent excess heat capacities of TiO₂ nanoparticles and water content and found that the specific heat of bare, water-free nanoparticles does not differ from that of bulk. The apparent effect of water on the specific heat arises from the smaller molecular weight of H₂O than of TiO₂, which leads to a larger number of atoms (and therefore oscillators) per gram of sample. This characterization of specific heat and water content provides a rationale to probe water heat capacity on the TiO₂ surface. Figure 1a shows the specific heat of water on 7 nm anatase nanoparticles, obtained by subtracting the bulk anatase heat capacity from that of nanoparticles containing water (sample AIII in ref 7). For comparison the specific heat of ice-Ih from nearly 0 to 300 K (extrapolated above 273 K) is also plotted in Figure 1a. Below

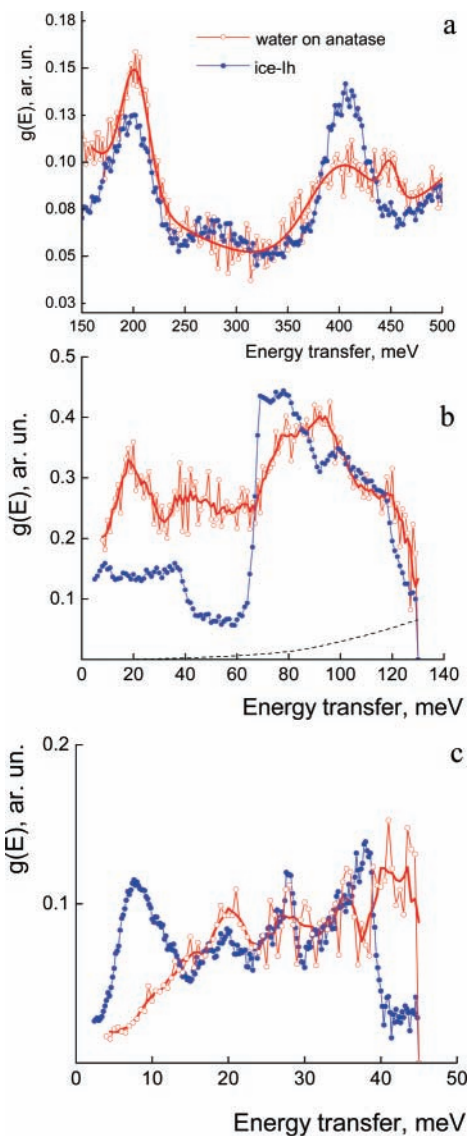


Figure 2. INS spectra of anatase 7 nm nanoparticles as compared to ice-Ih, obtained at $E_i = 600$ meV (a), $E_i = 140$ meV (b), and $E_i = 50$ meV (c). The solid thick lines are smoothed spectra. The dashed line shows multiphonon scattering. The bulk ice-Ih spectrum is from ref 3.

200 K, the specific heat curve for TiO_2 surface-confined water lies below that of hexagonal ice, but it rises above the ice curve at higher temperature. This yields a lower vibrational entropy S ($37.07 \text{ J K}^{-1} \text{ mol}^{-1}$ at 298.15 K) for the confined water than that of ice-Ih ($41.54 \text{ J K}^{-1} \text{ mol}^{-1}$ at 298.15 K) as shown in Figure 1b. This is because low temperature heat capacities ($T \rightarrow 0$) contribute heavily to the entropy as $S = \int_0^T C_p(T)/TdT$.³³

Inelastic Neutron Scattering Experiments. The INS spectrum of ice consists of low frequency intermolecular bands (translational and librational vibrations of water at 0–40 and 55–120 meV, respectively) and high frequency intramolecular vibrations (H–O–H bending modes at ~ 200 meV and O–H stretching modes at ~ 410 meV).

The amount of water on the surface is relatively low ($1.5 \times 10^{-5} \text{ mol of H}_2\text{O/m}^2$ per m^2 equivalent to 9 water molecules per nm^2), which results in a relatively low intensity and high noise level for the spectrum obtained at 600 meV (Figure 2a). Therefore, smoothed data are also shown in Figure 2 and compared to the spectrum of ice-Ih. It is clear that the typical features of the hexagonal ice-Ih spectrum are observed for the surface confined water.

The broad peak in the OH stretching region is centered at 400 meV, which is consistent with ice vibrations (Figure 2a). There is a narrow band centered at 449 meV (with $\text{fwhm} = 18$ meV) superimposed on the broad peak at 400 meV ($\text{fwhm} = 75$ meV), which extends to lower frequencies (down to 350 meV). The feature at ~ 450 meV is apparently related to OH stretching of either isolated hydroxyl group or water molecules without hydrogen bonds since higher frequencies (energies) indicate shorter and stronger covalent O–H bonds. From the fit to the OH stretching vibration band using two Gaussians, one can obtain the intensity ratio for peaks at 400 and 449 meV approximately as 1:6. Thus, we can estimate the ratio of the number of water molecules (H_2O) to the number of hydroxyls on the anatase surface as 3:1.

The low energy shoulder at 350–400 meV shows surprising softening of the OH stretching mode. This softening implies the existence of some longer (weaker) O–H covalent bonds and shorter O \cdots O distances (stronger O \cdots H–O hydrogen bonds) presumably between adjacent surface OH groups. Another possible scenario is that some physically adsorbed water molecules form two hydrogen bonds with surface oxygens O \cdots H–O–H \cdots O, resulting in weaker intramolecular water O–H bonds. The bending mode at ~ 200 meV, associated with molecular water, appears to be unchanged if compared to the ice-Ih spectrum (Figure 2a).

The part of the spectrum assigned to librational modes is characterized by a low energy cutoff. The peak observed at 70 meV for ice-Ih is not seen, possibly due to redistribution and broadening of the peak (Figure 2b). The INS spectrum of ice in the librational range is sensitive to changes in the tetrahedral arrangement of water molecules and typically interpreted in terms of distortions of tetrahedra. The $g(E)$ spectrum of ice-Ih has no vibrational modes between 40 and 65 meV, while the surface water spectrum has a rather intense band between 35 and 65 meV, which might be related to the interaction of water with TiO_2 , greatly enhanced by intense TiO_2 optical modes at around these energies. Because of strong interaction between anatase surface and water molecules or hydroxyl groups close to the TiO_2 surface, the corresponding hydrogen atoms can participate in vibrations of the TiO_2 matrix, so-called riding modes, and therefore, the eigenvectors of H_2O or OH groups interacting with TiO_2 can be significant in the VDOS spectra.

The translational modes in the energy range between 15 and 40 meV follow the ice-Ih spectrum profile (Figure 2c). The absence of an ice-Ih acoustic peak at 7 meV in the spectrum is striking. This convincingly shows that translational motion of water molecules is greatly suppressed, meaning that water is strongly bound to specific sites on the TiO_2 surface.

Vibrational Density of States and Heat Capacity Calculations. According to a study by Klug et al.,³¹ the heat capacity of ice-Ih is mostly vibrational and can be accurately estimated below 100 K from the INS spectra using the harmonic oscillator model

$$C_v = R \int_0^\infty \frac{g(\omega)(\hbar\omega/kT)^2 \exp(\hbar\omega/kT)}{[\exp(\hbar\omega/kT) - 1]^2} d\omega$$

where C_v is the isochoric molar heat capacity, R is the gas constant, \hbar is Planck's constant, ω is the phonon frequency, and k is Boltzmann's constant.

The anharmonic part of the specific heat associated with the thermal expansion $C_p - C_v = TV\alpha^2/\kappa_T$ (V is the molecular volume, α is the volume thermal expansion, and κ_T is the isothermal compressibility) is estimated to be negligible (0.025

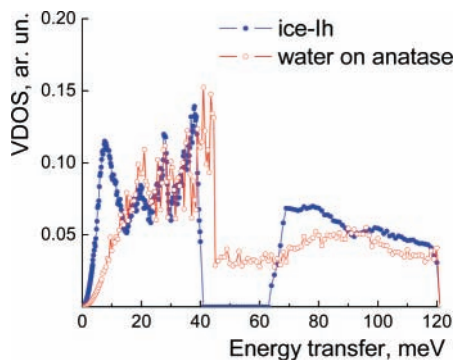


Figure 3. Vibrational density of states for water confined on the anatase surface and ice-Ih.

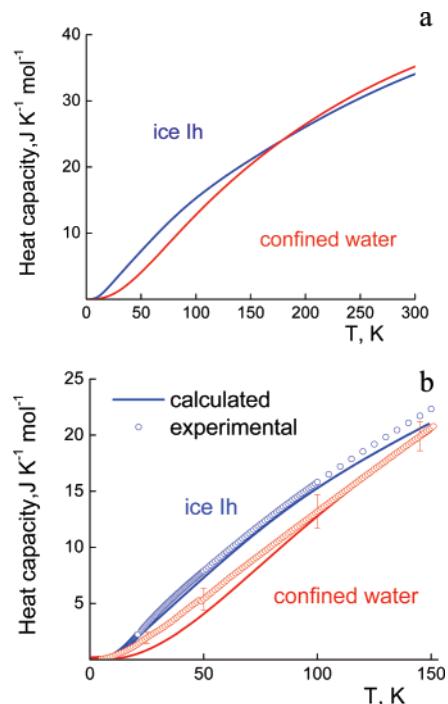


Figure 4. (a) C_v for bulk ice and TiO₂ surface confined water calculated from VDOS and (b) experimental C_p data for bulk ice and anatase confined water, as compared to calculated values from VDOS.

J mol⁻¹ K⁻¹) at 100 K³⁴, and the isobaric heat C_p capacity is virtually indistinguishable from the isochoric specific heat C_v . Above 100 K, the vibrational heat capacity of ice becomes noticeably anharmonic,³¹ and deviations of calculated heat capacity from the experimental values are expected.

To calculate the heat capacity from VDOS, INS spectra $g(E)$ were normalized to 6 (three degrees of freedom for each group of translational and librational modes) and approximated at low energies by the Debye law, $g(E) \sim E^2$ (Figure 3). For ice-Ih, the task of deconvoluting translational and librational bands is straightforward, while for water on the anatase surface it becomes nontrivial, contributing to higher calculation uncertainties. An energy of 45 meV was used in this study as a borderline between translational and librational bands.³⁵

Heat capacities for bulk and confined water, calculated from VDOS, are compared in Figure 4 with the experimental heat capacities from low temperature adiabatic calorimetric data (Figure 1a). The calculated heat capacities for ice-Ih are in good agreement with experimental values. The difference between experimental data and calculations for ice-Ih increases from 2.6 to 12% with decreasing temperature (from 100 to 10 K), giving rise to a mean deviation of 6.5%.

Discussion

The relationships between calculated heat capacities of nano- and bulk water bear remarkable resemblance to trends observed for calorimetric heat capacities (Figures 1a and 4a). Indeed, the heat capacity of water on the anatase surface, calculated from the VDOS, is lower than that of the bulk water in the low temperature range, resulting in lower entropy at room temperature for confined water as compared to that of the bulk.

The experimental and calculated values for the confined water are in satisfactory agreement with each other (Figure 4b), if the uncertainty associated with assuming zero excess heat capacity of anhydrous TiO₂ nanoparticles is taken into account. The error bars in Figure 4b for the calculated heat capacity of confined water include uncertainty arising from the assumption of zero excess heat capacity for anatase nanoparticles relative to bulk anatase (of the same order of magnitude as the uncertainty of the measured heat capacity) and uncertainty in the number of moles of water.⁷

The shifts of translational (acoustic) modes of surface water suggest restricted motion of water molecules near the TiO₂ surface. Strong interactions of this inner layer water via hydrogen bonds with the TiO₂ surface, which lead to acoustic vibrations at higher energies, cause acoustic modes of surface water to appear at higher frequencies than those of ice-Ih.

As indicated previously, the librational modes observed from 50 to 130 meV are sensitive to the short-range hydrogen bonding interactions that restrict the rotation of the water molecules. The translational modes of ice are not observed above 45 meV,³⁶ and therefore, a broad feature, seen between 50 and 70 in a gap of the ice spectrum, can be attributed to librations of surface-confined water. The center of gravity calculated for all librational modes of surface water (50–120 meV) shifts to lower energies, whereas the center of modes is not changed if calculated between 70 and 120 meV (the librational range of ice-Ih). This implies that the overall shift of librational modes to lower energies mostly results from the presence of the vibrations that are not observed in ice-Ih. A shift of librational bands to lower energies reflects softening of intermolecular hydrogen bonding.³⁶ This softening may be associated with distortions³⁷ in water tetrahedra and might be analogous to transformations observed in amorphous ice under pressure.^{34,38} As the pressure increases, C_p decreases at low temperatures, accompanied by an increase in the frequency of the translational modes and a consequent decrease in the intensity of VDOS at low energies.

Above 200 K, the experimental confined water specific heat rises above that of bulk ice-Ih. The calculations based on INS data show a similar crossover, attributed to the presence of vibrations between 40 and 60 meV, which are absent in ice-Ih. Our INS data were collected only at 4 K; thus, we have no direct evidence for possible changes in VDOS at higher temperatures. Faraone et al.²⁴ and Mamontov et al.^{1,2,26} suggested a dynamic (fragile-to-strong liquid) transition in confined water above its glass transition (180–200 K) in a number of systems (CeO₂, rutile TiO₂, SnO₂, MCM-41) at 210–220 K. We note that our observed crossover in heat capacity of water on the anatase surface and ice occurs in a similar temperature range. However, this crossover can be adequately modeled based on our 4 K VDOS (see Figure 4a) for the lightly hydrated anatase sample we measured by INS. Water on more highly hydrated anatase samples (hydration level comparable to that of the rutile TiO₂ sample in Mamontov et al.'s paper²⁶) showed a similar crossover in the experimental heat capacity relative to ice⁷ but with a much larger excess molar heat capacity than that calculated from the 4 K VDOS for the lightly hydrated sample.

Thus, it is not clear at this point whether an analogous dynamic transition plays a role in the energetics of water on anatase.

The softening of intramolecular stretching modes centered around 400 meV, seen as a shoulder in the spectrum of surface-confined water, is associated with a shorter hydrogen bond length O—H···O and stronger intermolecular hydrogen bonding, probably between surface hydroxyls and water molecules near the surface.

Conclusion

INS experiments, even on a limited amount of a TiO₂ sample, clearly reveal the vibrational density of states of water. Modes of water molecules and surface hydroxyls have been observed, confirming our previous studies^{5,6} that indicated a mixed character of water adsorption (dissociative and molecular) on nanophase TiO₂. We observed shifts or redistribution of low energy modes (translational vibrations) to higher energy and softening of librational modes, indicating very restricted dynamics of surface water and a distorted network of tetrahedra. This combined INS and calorimetry study supports our previously proposed finding⁶ that the heat capacity and entropy of water molecules in a confined geometry can be lower than those in bulk due to stronger interactions at the interface.

Acknowledgment. The U.S. Department of Energy provided support under Grant DE FG03 01ER15237. The work performed at Argonne National Laboratory is supported by the U.S. DOE-BES under Contract W-31-109-ENG-38. We are grateful to L. Jirik for assistance with neutron scattering experiments at IPNS.

Supporting Information Available: Contributions of translational and librational bands to heat capacities of ice-Ih and confined water are calculated using VDOS. As one can see, the C_p for ice-Ih, due to only translational modes, is larger than that for anatase water at all temperatures, while the contributions from the librational modes are smaller. A gradual increase of the librational contribution to C_p for anatase water (larger than for ice-Ih) with temperature results in total C_p being larger for anatase water than for ice-Ih above ~180 K. This material is available free of charge via the Internet at <http://pubs.acs.org>.

References and Notes

- Mamontov, E. *J. Chem. Phys.* **2005**, *123*, 024706–9.
- Mamontov, E. *J. Chem. Phys.* **2005**, *123*, 171101–4.
- Kolesnikov, A. I.; Zanolli, J.-M.; Loong, C.-K.; Thiagarajan, P.; Moravsky, A. P.; Loutfy, R. O.; Burnham, C. *J. Phys. Rev. Lett.* **2004**, *93*, 035503–4.
- Trofymuk, O.; Levchenko, A. A.; Navrotsky, A. *J. Chem. Phys.* **2005**, *123*, 194509–6.
- Li, G. S.; Li, L. P.; Boerio-Goates, J.; Woodfield, B. F. *J. Am. Chem. Soc.* **2005**, *127*, 8659–8666.
- Levchenko, A. A.; Li, G.; Boerio-Goates, J.; Woodfield, B. F.; Navrotsky, A. *Chem. Mater.* **2006**, *18*, 6324–6332.
- Boerio-Goates, J.; Li, G. S.; Li, L. P.; Walker, T. F.; Parry, T.; Woodfield, B. F. *Nano Lett.* **2006**, *6*, 750–754.
- Korn, D. *J. Phys. Chem.* **1988**, *49*, 769–779.
- Hellstern, E.; Fecht, H. J.; Fu, Z.; Johnson, W. L. *J. Appl. Phys.* **1989**, *65*, 305–310.
- Kramer, W.; Noelting, J. *Acta Metall.* **1972**, *20*, 1353–1359.
- Lu, K.; Wang, J. T.; Wei, W. D. *Scr. Metall. Mater.* **1991**, *25*, 619–623.
- Rupp, J.; Birringer, R. *Phys. Rev. B* **1987**, *36*, 7888–7890.
- Stewart, G. R. *Phys. Rev. B* **1977**, *15*, 1143–1150.
- Chen, Y. Y.; Yao, Y. D.; Hsiao, S. S.; Jen, S. U.; Lin, B. T.; Lin, H. M. *Phys. Rev. B* **1995**, *52*, 9364–9370.
- Volokitin, Y.; Sinzig, J. L.; de Jongh, J.; Schmid, G.; Vargaftik, M. N.; Moiseev, I. I. *Nature (London, U.K.)* **1996**, *384*, 621–623.
- Wang, C. R.; Chen, Y. Y.; Yao, Y. D.; Pan, S. F.; Ho, J. C.; Chang, C. L.; H. C. L. *Phys. B* **2000**, *284–288*, 1738–1739.
- Herr, U.; Samwer, G. K. *Philos. Mag. A* **1998**, *77*, 641–652.
- Hoch, M.; Vernardakis, T. *Rev. Int. Hautes Temp. Refract.* **1976**, *13*, 75–82.
- Terwilliger, C. D.; Chiang, Y.-M. *J. Amer. Cer. Soc.* **1995**, *78*, 2045–2055.
- Kolesnikov, A. I.; Li, J. C.; Parker, S. F. *J. Mol. Liq.* **2002**, *96–97*, 317–325.
- Bellissent-Funel, M. C. *Eur. Phys. J. E* **2003**, *12*, 83–92.
- Corrado, C.; Crupi, V.; Majolino, D.; Parker, S. F.; Venuti, V.; Wanderlingh, U. *J. Phys. Chem. A* **2006**, *110*, 1190–1195.
- Zanolli, J. M.; Bellissent-Funel, M. C.; Chen, S. H.; Kolesnikov, A. I. *J. Phys.: Condens. Matter* **2006**, *18*, 2299–2304.
- Faraone, A.; Liu, L.; Mou, C. Y.; Yen, C. W.; Chen, S. H. *J. Chem. Phys.* **2004**, *121*, 10843–10846.
- Loong, C. K.; Iton, L. E.; Ozawa, M. *Phys. B* **1995**, *213*, 640–642.
- Mamontov, E.; Vlcek, L.; Wesolowski, D. J.; Cummings, P. T.; Wang, W.; Anovitz, L. M.; Rosenqvist, J.; Brown, C. M.; Sakai, V. G. *J. Phys. Chem. C* **2007**, *111*, 4328–4341.
- Loong, C. K.; Richardson, J. W.; Ozawa, M. *J. Catal.* **1995**, *157*, 636–644.
- Brunauer, S.; Emmett, P. H.; Teller, E. *J. Am. Chem. Soc.* **1938**, *60*, 309–319.
- Sing, K. S. W.; Everett, D. H.; Haul, R. A. W.; Moscou, L.; Pierotti, R. A.; Rouquerol, J.; Siemieniewska, T. *Pure Appl. Chem.* **1985**, *57*, 603–619.
- Kolesnikov, A. I.; Natkaniec, I.; Antonov, V. E.; Belash, I. T.; Fedotov, V. K.; Krawczyk, J.; Mayer, J.; Ponyatovsky, E. G. *Phys. B* **1991**, *174*, 257–261.
- Klug, D. D.; Whalley, E.; Svensson, E. C.; Root, J. H.; Sears, V. F. *Phys. Rev. B* **1991**, *44*, 841–844.
- Stevens, R.; Boerio-Goates, J. *J. Chem. Thermodyn.* **2004**, *36*, 857–863.
- Ott, J. B.; Boerio-Goates, J. *Chemical Thermodynamics: Principles and Applications*; Academic Press: San Diego, 2000.
- Johari, G. P.; Andersson, O. *Phys. Rev. B* **2006**, *73*, 094202–6.
- Kolesnikov, A. I.; Sinityn, V. V.; Ponyatovsky, E. G.; Natkaniec, I. Smirnov, L. S. *Phys. B* **1995**, *213*, 474–476.
- Kolesnikov, A. I.; Sinityn, V. V.; Ponyatovsky, E. G.; Natkaniec, I.; Smirnov, L. S.; Li, J. C. *J. Phys. Chem. B* **1997**, *101*, 6082–6086.
- Guillot, B.; Guissani, Y. *J. Chem. Phys.* **2003**, *119*, 11740–11752.
- Subbotin, O. S.; Belosludov, V. R.; Inerbaev, T. M.; Belosludov, R. V. Kawazoe, Y. *Comput. Mater. Sci.* **2006**, *36*, 253–257.